DECLASSIFIED

TECHNICAL MEMORANDUM X-895

LOW-SPEED EFFECTS OF HIGH-LIFT DEVICES ON THE

AERODYNAMIC CHARACTERISTICS OF A SUPERSONIC

TRANSPORT MODEL WITH OUTBOARD TAILS

By William C. Sleeman, Jr., Edward J. Ray,
and Paul G. Fournier

Langley Research Center
Langley Station, Hampton, Va.

NATIONAL AERONAUTICS AND SPACE ADMINISTRATION

CONFIDENTIAL

NATIONAL AERONAUTICS AND SPACE ADMINISTRATION

TECHNICAL MEMORANDUM X-895

LOW-SPEED EFFECTS OF HIGH-LIFT DEVICES ON THE AERODYNAMIC

CHARACTERISTICS OF A SUPERSONIC TRANSPORT

MODEL WITH OUTBOARD TAILS*

By William C. Sleeman, Jr., Edward J. Ray,
and Paul G. Fournier

SUMMARY

A low-speed investigation has been made to study the effects of high-lift devices (leading-edge and trailing-edge flaps) on the longitudinal stability and trim characteristics of an outboard-tail supersonic transport configuration. The effects on the pitch characteristics of varying the gap between the wing and flaps were also investigated. A brief study was made to determine the effect of leading-edge-flap deflection on the lateral stability derivatives of the model.

The results indicated that there was an appreciable loss in longitudinal stability in going from low to moderate lift coefficients for the model with the flaps undeflected. Deflection of the trailing-edge flaps caused further losses of stability, and the model was highly unstable at lift coefficients above about 0.8. Additional development work would be needed, therefore, to provide satisfactory low-speed longitudinal stability characteristics.

INTRODUCTION

The National Aeronautics and Space Administration has investigated a number of supersonic transport configurations as part of a research program to assess the technical and economic feasibility of developing a supersonic commercial air transport (SCAT). One part of the present research effort, in the supersonic region, is to develop a configuration which is capable of achieving cruise speeds of Mach 2 to Mach 3 economically for both domestic and trans-Atlantic travel. Existing airline facilities, such as landing fields and approach systems, dictate that in addition to this requirement, a suitable supersonic transport must possess subsonic capabilities comparable to, or exceeding, those of present-day subsonic transports. A variety of design concepts, including both fixed-geometry and variable-geometry wings, have been evaluated in the effort to satisfy the prerequisites of an acceptable supersonic transport. Results of other wind-tunnel

---

*Title, Unclassified.

investigations dealing with both the subsonic and supersonic characteristics of supersonic transport configurations are presented in reference 1 to 6.

The present investigation is concerned with a supersonic transport configuration having the tail surfaces located outboard of the wing tips (designated SCAT 2B). The outboard-tail transport configuration was first investigated as an outgrowth of work accomplished on supersonic bomber configurations having tail surfaces mounted on slender bodies attached to the wing tips. Experimental results for these outboard-tail configurations at supersonic speeds are presented in reference 2. Low-speed test results which show effects of wing-flap deflection were obtained on a simplified outboard-tail model and are presented in reference 7. Data obtained from previous investigations of outboard-tail models at supersonic speeds have indicated that relatively high lift-drag ratios could be obtained for trimmed conditions over a large range of low-lift static margins. However, static longitudinal instability occurred at moderate lift coefficients at both subsonic and supersonic speeds (refs. 8 and 9). In the present investigation emphasis was placed on the application of high-lift devices to an outboard-tail supersonic transport configuration to determine the longitudinal stability and trim and the maximum lift coefficient available for landing.

This investigation was made in the Langley high-speed 7- by 10-foot tunnel over an angle-of-attack range from approximately -1° to 25°. The model had a 60° sweptback wing with an aspect ratio of 1.22 and was equipped with leading-edge flaps and extended trailing-edge flaps. The tests were conducted at a Reynolds number of approximately 2.69×10^6, based on the mean aerodynamic chord. The effects of high-lift devices on the longitudinal stability characteristics and maximum lift coefficient available for landing were assessed by applying leading-edge flaps and trailing-edge flaps to the basic model. In addition, gap widths between the flaps and wing were varied to measure the effect on the pitch characteristics of the model. Lateral stability derivatives were determined for the model with the trailing-edge flaps undeflected.

SYMBOLS

The data of this investigation are referred to the system of axes illustrated in figure 1. Moment coefficients are referred to a point located 59.63 inches from the nose of the model. The coefficients are based on the sum of the wing and horizontal-tail areas including the area intercepted by the fuselage and the bodies at the wing tips. The reference chord used in the reduction of data is the mean aerodynamic chord based on composite wing and horizontal tail. Coefficients and symbols are defined as follows:

C_L lift coefficient, $\dfrac{\text{Lift}}{qS}$

C_D drag coefficient, $\dfrac{\text{Drag}}{qS}$

C_m pitching-moment coefficient, $\dfrac{\text{Pitching moment}}{qS\bar{c}}$

C_l rolling-moment coefficient, $\dfrac{\text{Rolling moment}}{qSb}$

C_n yawing-moment coefficient, $\dfrac{\text{Yawing moment}}{qSb}$

C_Y side-force coefficient, $\dfrac{\text{Side force}}{qS}$

C_{l_β} effective-dihedral parameter, $\left(\dfrac{\Delta C_l}{\Delta \beta}\right)_{\beta=\pm 4^\circ}$

C_{n_β} directional-stability parameter, $\left(\dfrac{\Delta C_n}{\Delta \beta}\right)_{\beta=\pm 4^\circ}$

C_{Y_β} side-force parameter, $\left(\dfrac{\Delta C_Y}{\Delta \beta}\right)_{\beta=\pm 4^\circ}$

b span of wing plus horizontal tails, ft

c chord of wing, ft

c_n chord of leading-edge flap measured in streamwise direction, ft

$\bar{c}$ mean aerodynamic chord of wing plus horizontal tail, ft

$\bar{c}_h$ mean aerodynamic chord of horizontal tail, ft

$\bar{c}_w$ mean aerodynamic chord of wing alone, ft

i_t horizontal-tail incidence angle relative to center line of fuselage (positive when trailing edge is down), deg

q free-stream dynamic pressure, lb/sq ft

S area of wing plus area of horizontal tails, sq ft

α angle of attack of fuselage center line, deg

β angle of sideslip, deg

δ_f deflection of extended trailing-edge flap (positive when trailing edge is down), deg

δ_n deflection of leading-edge flap with respect to wing chord in free-stream direction (positive when leading edge is down), deg

MODEL AND APPARATUS

Figure 2(a) illustrates the general arrangement of the basic model used in this investigation, and the pertinent geometric characteristics of the model lifting surfaces are presented in table I. The fuselage and wing-tip bodies were made of mahogany and aluminum, and the wing, tail surfaces, and flaps were made of aluminum.

The wing of the model had modified double-wedge sections, a leading-edge sweepback of 60°, and an aspect ratio of 1.22. The wing was made up of three parts of equal chord length: the forward and after portions of the wing were wedges and the center portion had a constant thickness of $0.02\bar{c}_w$. The wing contained no twist but had a dihedral angle of -5°. The wing was inclined to the fuselage center line at an incidence angle of 2°, leading edge up. Provisions were made to replace the forward $0.24\bar{c}_w$ portion of the leading edge of the wing with single-wedge flaps with an aspect ratio of 1.75. When deflected the leading-edge flaps were fixed to the wing at an angle of 30°, leading edge down, by means of brackets oriented in the streamwise direction. Extended trailing-edge flaps were provided which could be attached by brackets to the trailing edge of the wing at angles of 30° or 45°, trailing edge down. The trailing-edge flaps had a constant chord and an aspect ratio of 2.32. The leading-edge flap and trailing-edge flap are illustrated in figure 2(b).

The wing-tip bodies were inclined 1° nose up with respect to the fuselage center line and had a fineness ratio of 14.67. The after end of the vertical tails was mounted even with the end of the wing-tip bodies and the vertical tails were toed out 1.5° with respect to the fuselage center line. The outboard side of the vertical tails was on the outboard side of the wing-tip bodies and was flat to minimize the gap between the vertical and horizontal tail surfaces when the horizontal tail was deflected. The horizontal tails pivoted about the $0.25\bar{c}_h$ line through a deflection range from 0° to -15°. Dihedral of the horizontal tail was -3°.

The model was mounted in the Langley high-speed 7- by 10-foot tunnel on a variable-angle sting which was inserted into the engine pack at the rear of the fuselage. Provision was made for internal flow through the two air ducts on the sides of the fuselage. The forces and moments acting on the model were measured with a six-component strain-gage balance attached to the sting within the fuselage.

TESTS AND CORRECTIONS

The investigation was made at a dynamic pressure of 50.0 pounds per square foot, which corresponds to an airspeed of about 140 miles per hour. The test conditions produced a Reynolds number of approximately 2.69×10^6 based on the mean

aerodynamic chord of the combined wing and horizontal tail. The test angle-of-attack range was from approximately -1° to 25°. Lateral-stability tests were conducted through a range of angle of attack at sideslip angles of 4° and -4° with a horizontal-tail incidence of -5°.

All angles of attack and sideslip have been corrected for deflection of the balance and sting combination due to aerodynamic load. The usual jet-boundary and blockage corrections have not been applied to the data inasmuch as these corrections are believed to be small for the present perforated-slot configuration used in the Langley high-speed 7- by 10-foot tunnel. No measurements were made of internal flow through the ducts, and the drag coefficients have been corrected for balance-chamber pressure only.

RESULTS

The results obtained in this investigation indicated that there was an appreciable loss in longitudinal stability in going from low to moderate lift coefficients for the model with the flaps undeflected. Deflection of the trailing-edge flaps caused further losses of stability, and the model was highly unstable at lift coefficients above about 0.8. Additional development work would be needed, therefore, to provide satisfactory low-speed longitudinal stability characteristics.

The figures presenting the results are as follows:

Figure

Aerodynamic characteristics in pitch of the basic model.
$\delta_f = 0°$; $\delta_n = 0°$ 3

Aerodynamic characteristics in pitch of the model with trailing-edge flaps deflected. $\delta_f = 45°$; $\delta_n = 0°$ 4

Aerodynamic characteristics in pitch of the model with leading-edge and trailing-edge flaps deflected. $\delta_f = 45°$; $\delta_n = 30°$ 5

Aerodynamic characteristics in pitch of the model with leading-edge and trailing-edge flaps deflected. $\delta_f = 30°$; $\delta_n = 30°$ 6

Effect of sealing the gap at the wing leading-edge flaps on the aero-dynamic characteristics in pitch of the model. $\delta_f = 0°$; $\delta_n = 30°$;
$i_t = -5°$ 7

Effect of gap width at the trailing-edge flaps on the aerodynamic characteristics in pitch of the model with the leading-edge flaps deflected. $\delta_f = 30°$; $\delta_n = 30°$; $i_t = -15°$ 8

Effect of leading-edge flap deflection on the lateral stability derivatives of the model. $\delta_f = 0°$; $i_t = -5°$ 9

Langley Research Center,
    National Aeronautics and Space Administration,
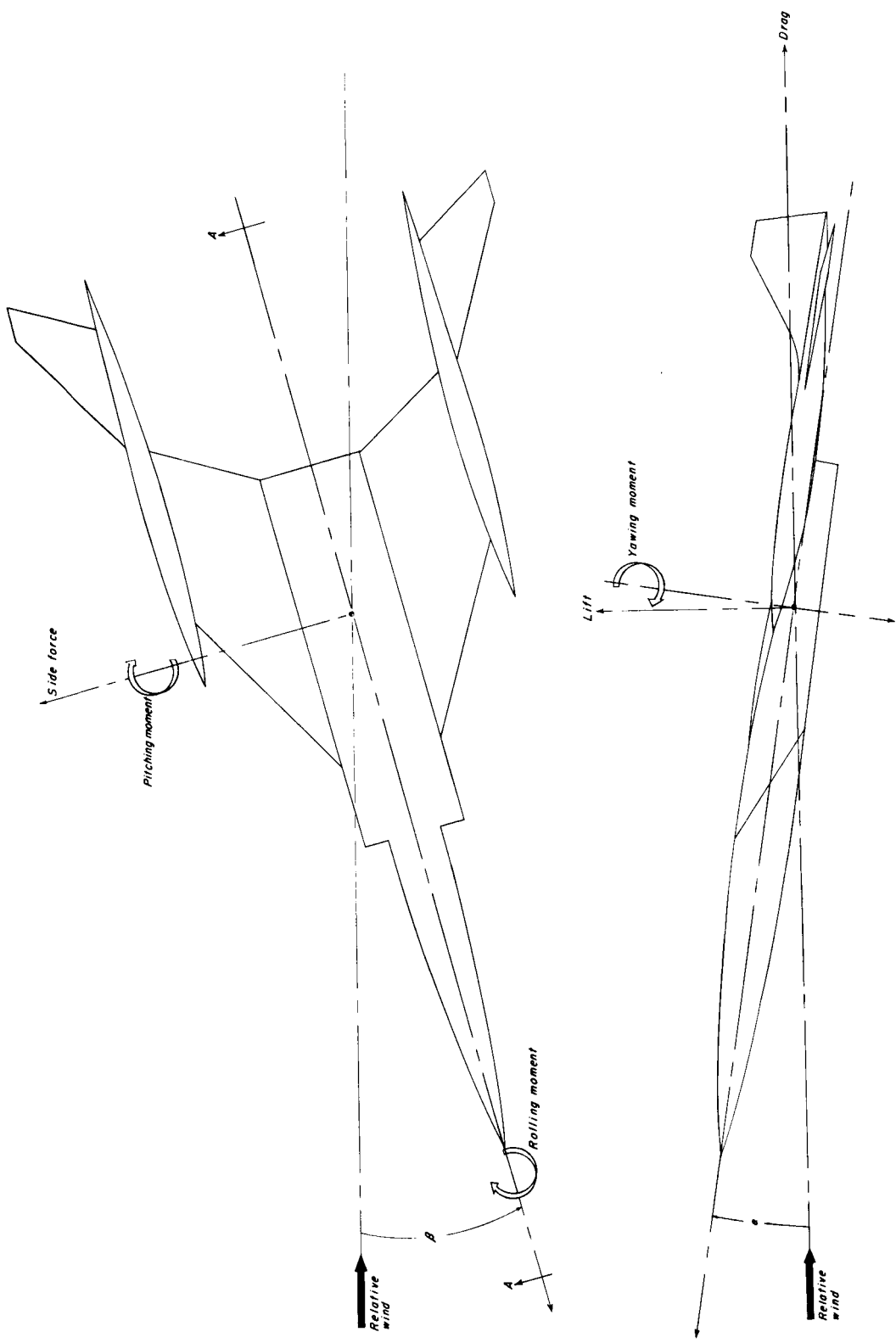   Langley Station, Hampton, Va., July 1963.

REFERENCES

1. Vogler, Raymond D., and Turner, Thomas R.: Exploratory Low-Speed Wind-Tunnel Stability Investigation of a Supersonic Transport Configuration With Variable-Sweep Wings. NASA TM X-597, 1961.

2. Sleeman, William C., Jr., Reed, James D., and Gainer, Thomas G.: Aerodynamic Characteristics of a Transport Airplane Configuration Having Tail Surfaces Located Outboard of the Wing Tips at Mach Numbers of 2.30, 2.96, 3.95, and 4.63. NASA TM X-556, 1961.

3. Sleeman, William C., Jr., and Robins, A. Warner: Low-Speed Investigation of the Aerodynamic Characteristics of a Variable-Sweep Supersonic Transport Configuration Having a Blended Wing and Body. NASA TM X-619, 1962.

4. Ward, Robert J., and McKee, John W.: Low-Speed Aerodynamic Stability and Control Characteristics of a Cambered Fuselage, Variable-Sweep Supersonic Transport Configuration. NASA TM X-632, 1962.

5. Sleeman, William C., Jr.: Low-Speed Investigation of the Effects of Horizontal Tail Height and Extension of the Wing-Root Leading-Edge Sections on a Variable-Sweep Supersonic Transport Configuration. NASA TM X-681, 1962.

6. Vogler, Raymond D.: Low-Speed Wind-Tunnel Stability Investigation of a Supersonic Transport Model With Variable-Sweep Wings Equipped With High-Lift Devices. NASA TM X-728, 1962.

7. Hayes, William C., Jr., and Sleeman, William C., Jr.: Low-Speed Investigation of the Effects of Wing Flap Deflection and Horizontal-Tail Configuration on the Longitudinal Aerodynamic Characteristics of an Airplane Configuration Having Tail Surfaces Outboard of the Wing Tips. NASA TM X-333, 1960.

8. Church, James D., Hayes, William C., Jr., and Sleeman, William C., Jr.: Investigation of Aerodynamic Characteristics of an Airplane Configuration Having Tail Surfaces Outboard of the Wing Tips at Mach Numbers of 2.30, 2.97, and 3.51. NACA RM L58C25, 1958.

9. Hayes, William C., Jr., and Sleeman, William C., Jr.: Low-Speed Investigation of the Effects of Horizontal-Tail Area and Wing Sweep on the Static Longitudinal Stability and Control Characteristics of an Airplane Configuration Having Tail Surfaces Outboard of the Wing Tips. NASA MEMO 6-11-59L, 1959.

TABLE I.- GEOMETRIC CHARACTERISTICS OF MODEL

Wing plus horizontal tails (used in reduction of data):
    Area, sq ft 7.2406
    Span, ft 4.2547
    Mean aerodynamic chord, ft 2.1010

Wing:
    Area, sq ft 6.1356
    Span, ft 2.7395
    Mean aerodynamic chord, ft 2.3324
    Aspect ratio 1.2232
    Taper ratio 0.4781
    Leading-edge sweepback, deg 60.00
    Trailing-edge sweepback, deg 30.00
    Dihedral, deg . . . . -5.00
    Incidence, deg 2.00
    Airfoil section . . . . $2\frac{1}{2}$ percent thick

Horizontal tail (one panel):
    Area, sq ft 0.5525
    Span, ft 0.7576
    Mean aerodynamic chord, ft 0.8165
    Aspect ratio 1.0388
    Taper ratio 0.2500
    Leading-edge sweepback, deg 60.00
    Trailing-edge sweepback, deg 30.00
    Airfoil section . . . . $2\frac{1}{2}$- percent-thick plate with rounded
                                                        leading edge and beveled trailing edge

Vertical tail (one panel):
    Area, sq ft 0.4667
    Span, ft 0.5850
    Mean aerodynamic chord, ft 0.9005
    Aspect ratio 0.7332
    Taper ratio 0.2331
    Leading-edge sweepback, deg 55.00
    Airfoil section . . . . $2\frac{1}{2}$- percent-thick plate with trailing
                                                          edge beveled on inboard side

Extended trailing-edge flap (one panel):
    Area, sq ft 0.3530
    Span, ft 0.9050
    Aspect ratio 2.3202
    Taper ratio 1.0000
    Airfoil section . . . . 5-percent-thick airfoil with flat underside

Leading-edge flap (one panel):
    Area, sq ft 0.4174
    Span, ft 0.8542
    Mean aerodynamic chord, ft 0.4982
    Aspect ratio 1.7478
    Taper ratio 0.6113
    Airfoil section . . . . Single-wedge extension of wing leading edge

8

Side force

Pitching moment

Relative wind

Rolling moment

B

A

A

Drag

Yawing moment

Lift

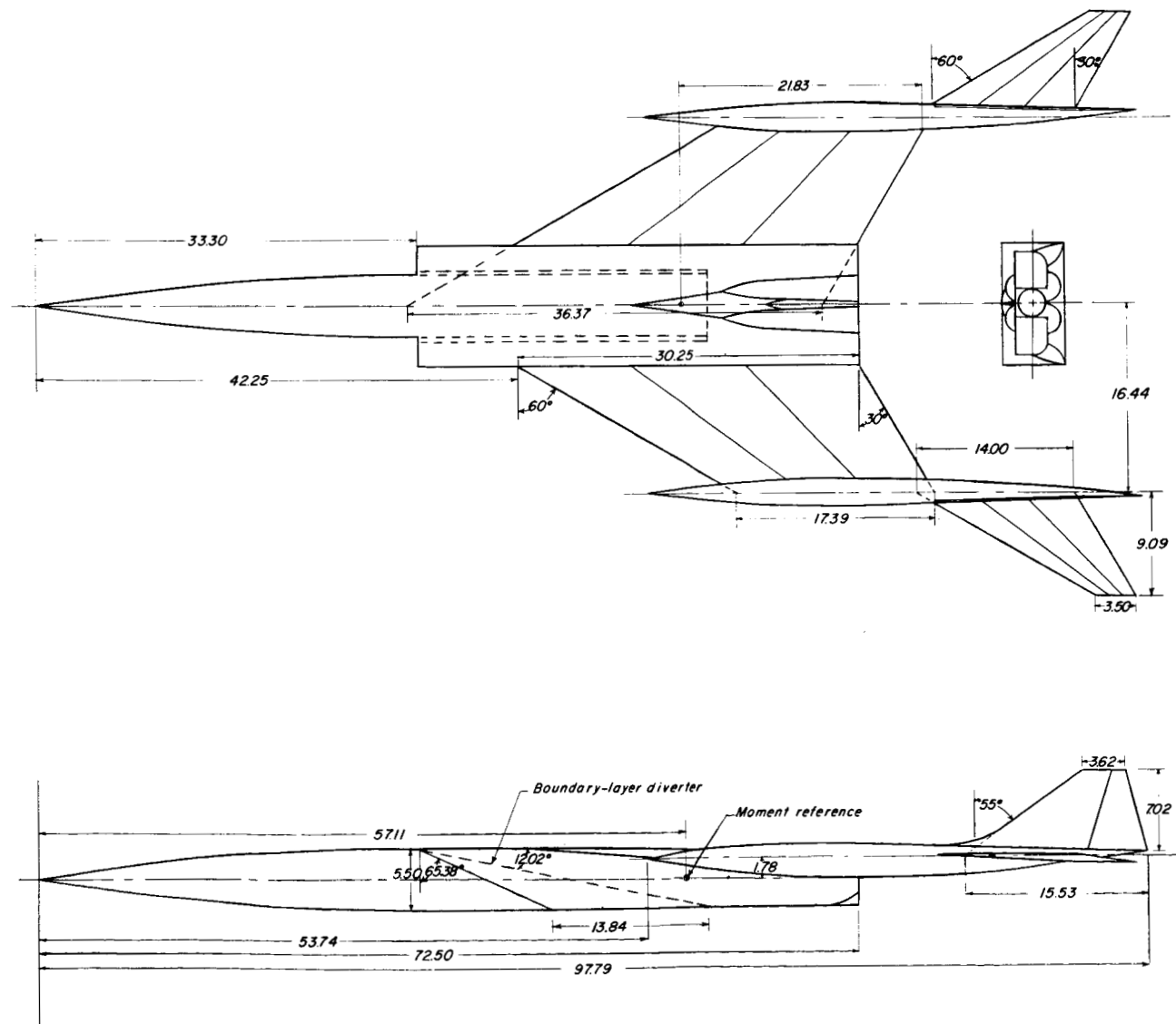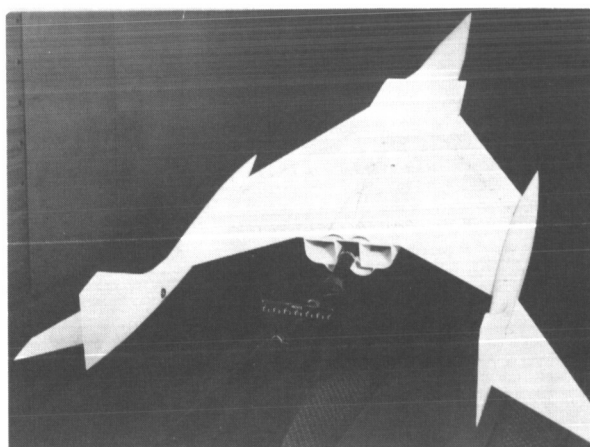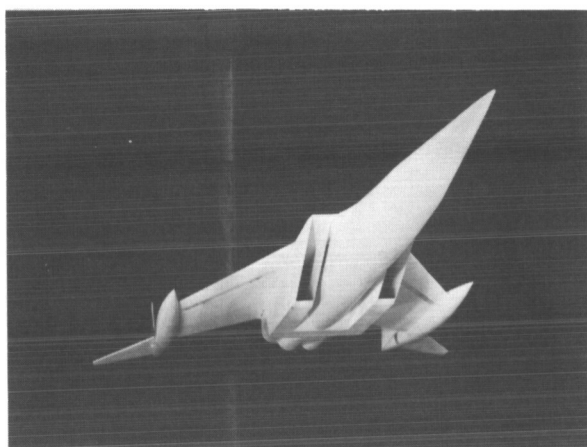Relative wind

View A-A

Figure 1.- System of axes.
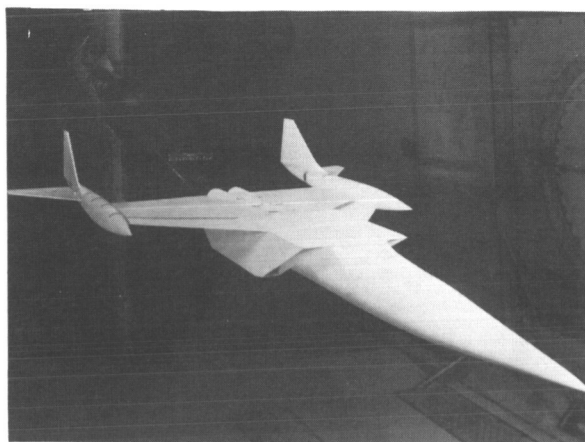
(a) General arrangement.

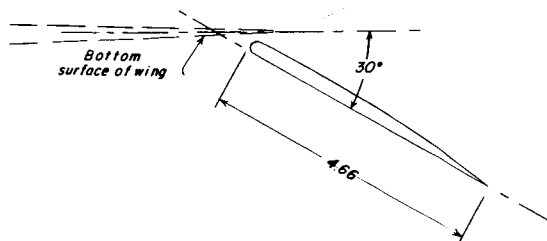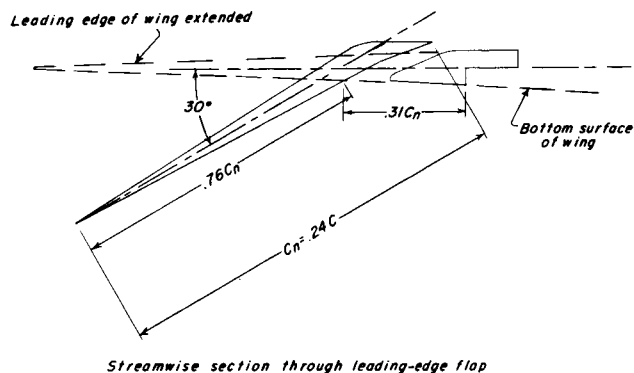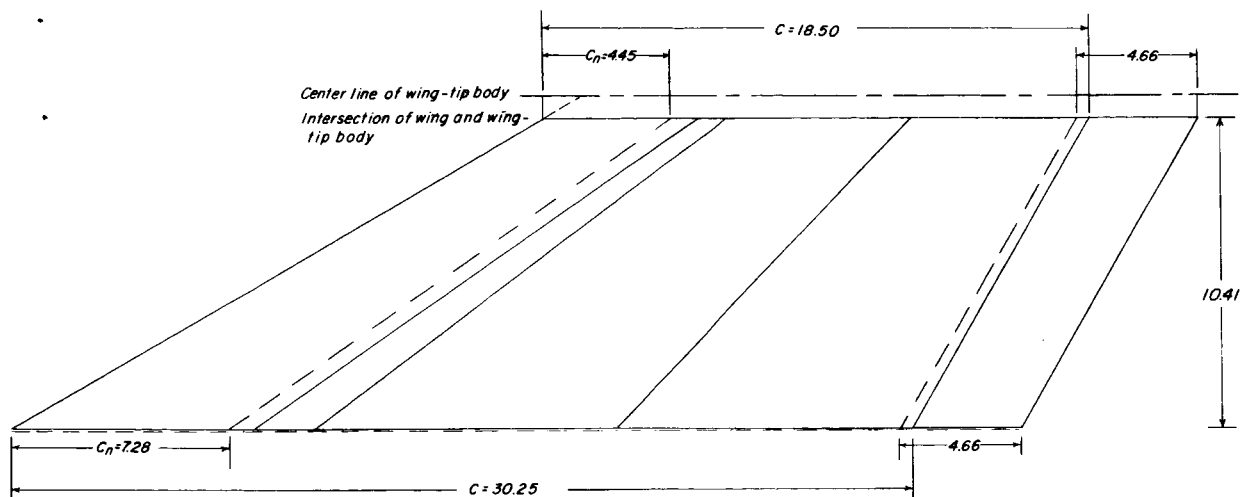Figure 2.- Outboard-tail supersonic transport configuration.

(a) Concluded.   L-63-4721

Figure 2.- Continued.

Streamwise section through leading-edge flap

Streamwise section through trailing-edge flap

(b) Details of wing flaps.

Figure 2.- Concluded.
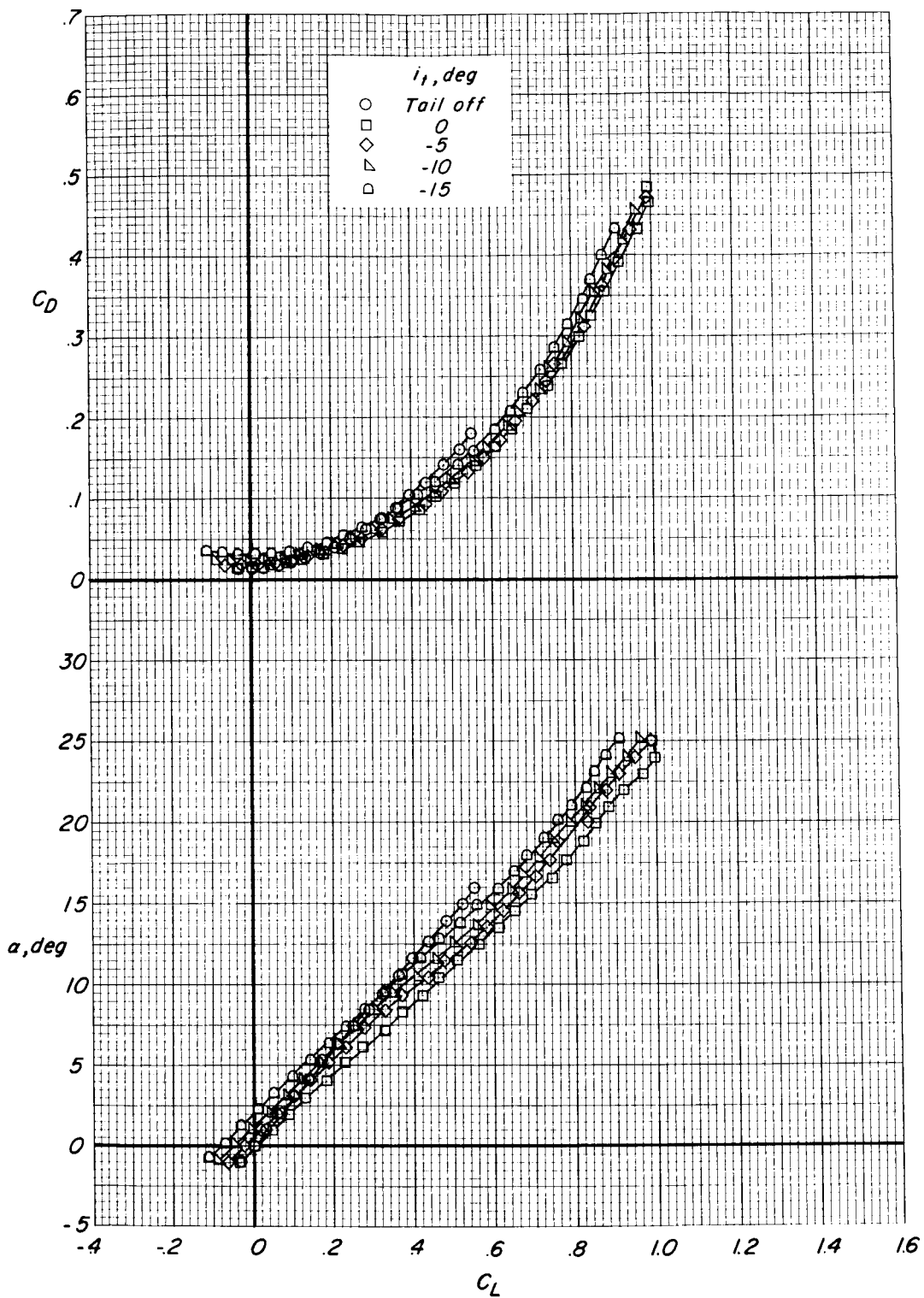
Figure 3.- Aerodynamic characteristics in pitch of the basic model. $\delta_f = 0^\circ$; $\delta_n = 0^\circ$.
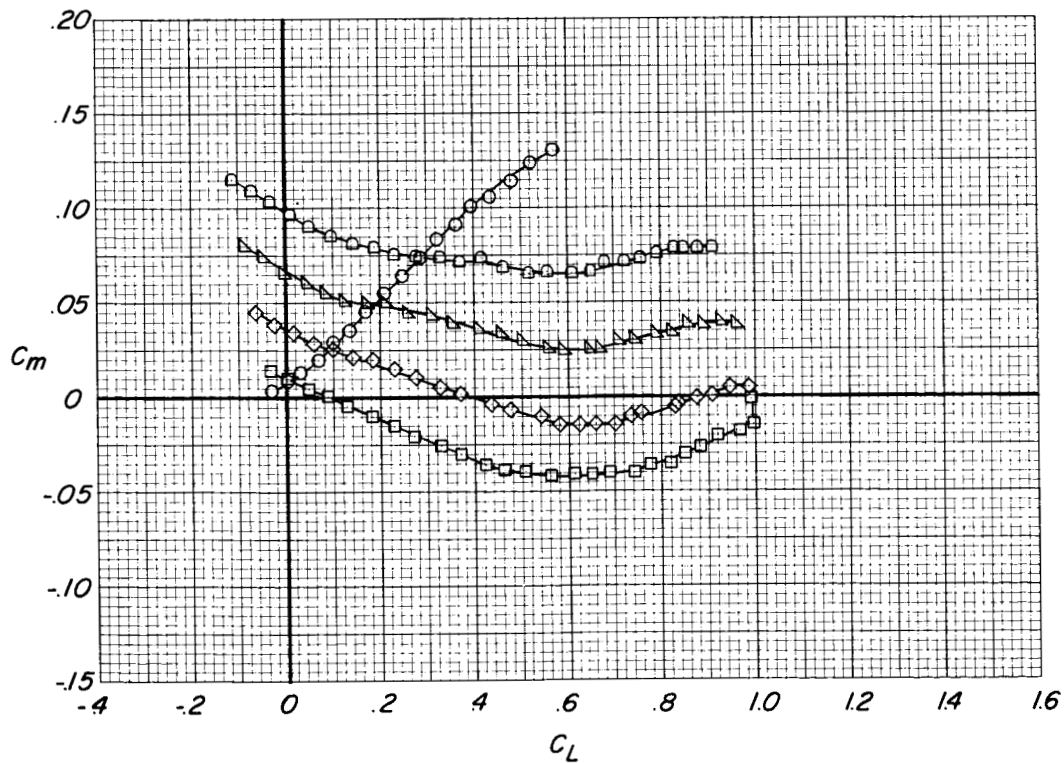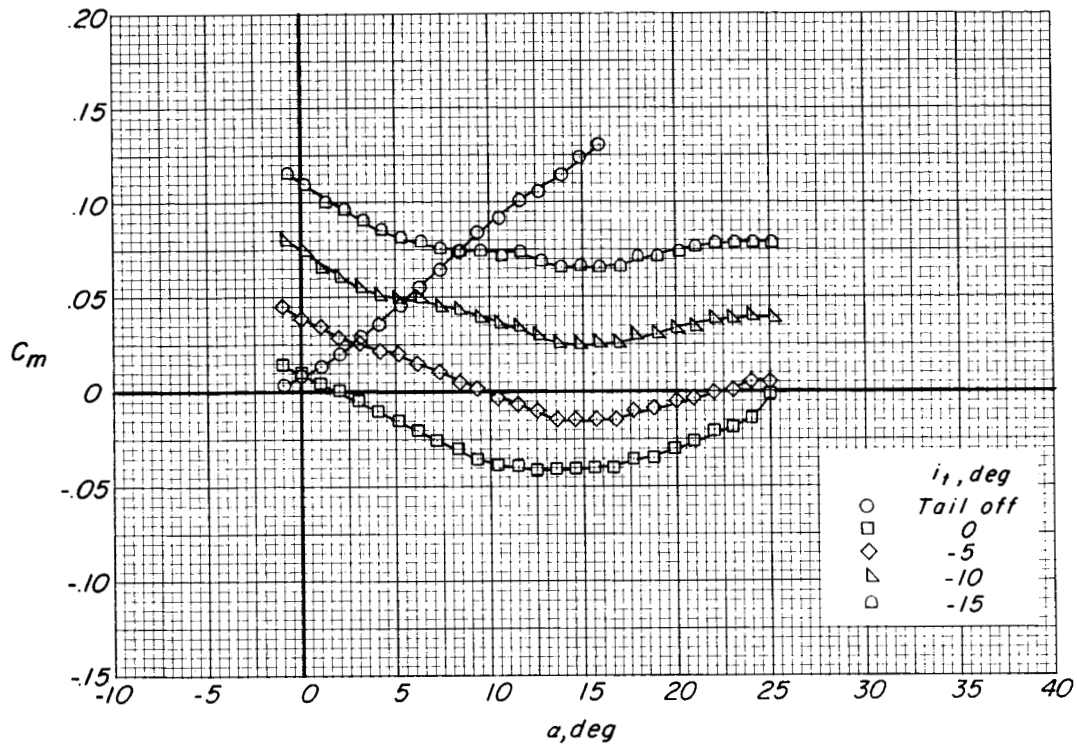
Figure 3.- Concluded.
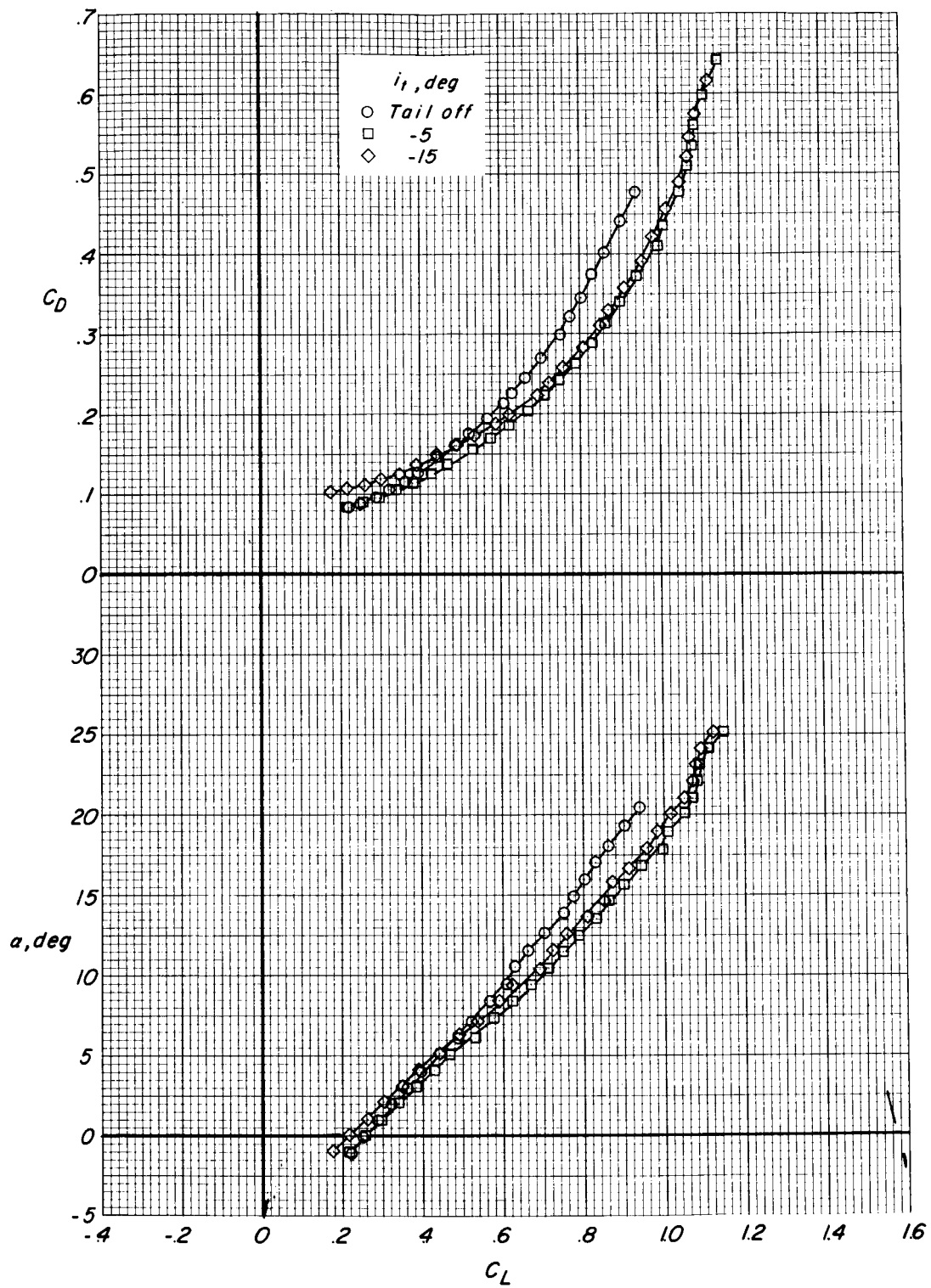
Figure 4.- Aerodynamic characteristics in pitch of the model with trailing-edge flaps deflected. $\delta_f = 45°$; $\delta_n = 0°$.
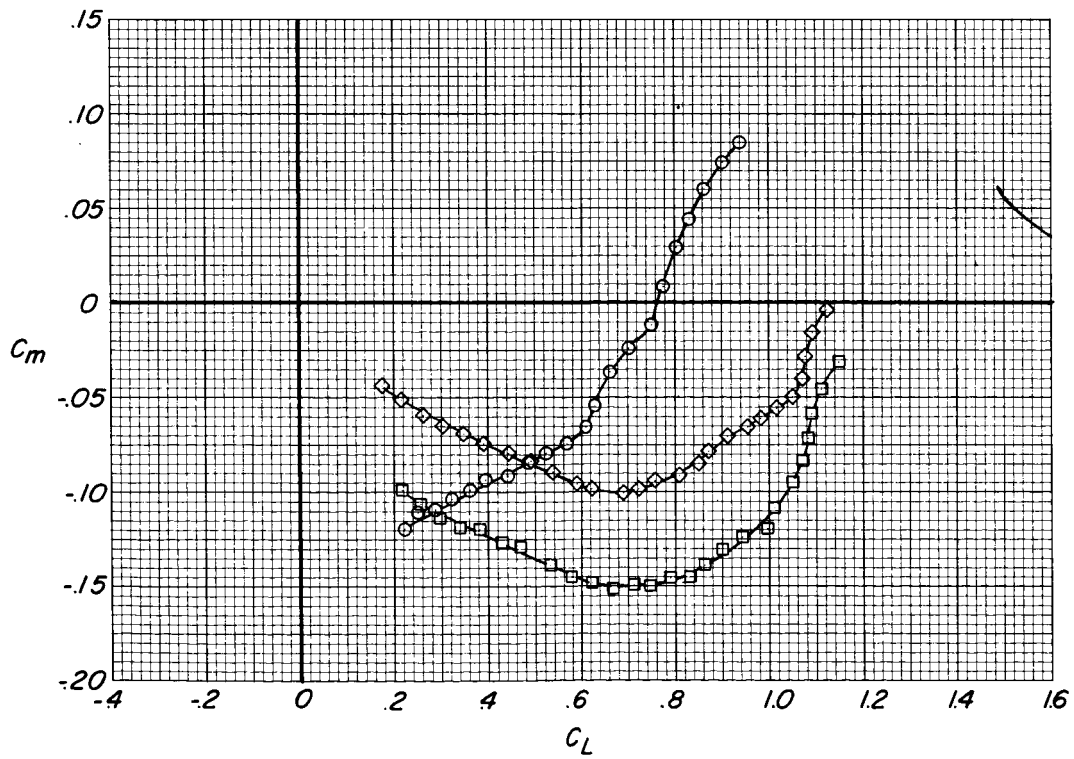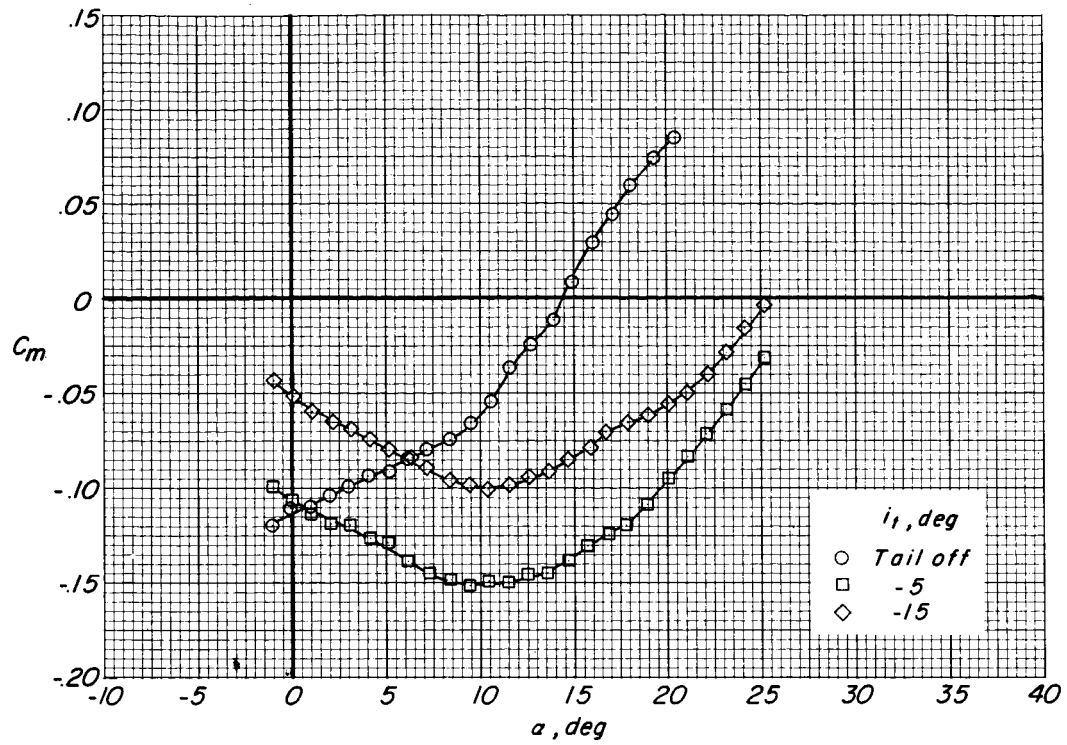
Figure 4.- Concluded.
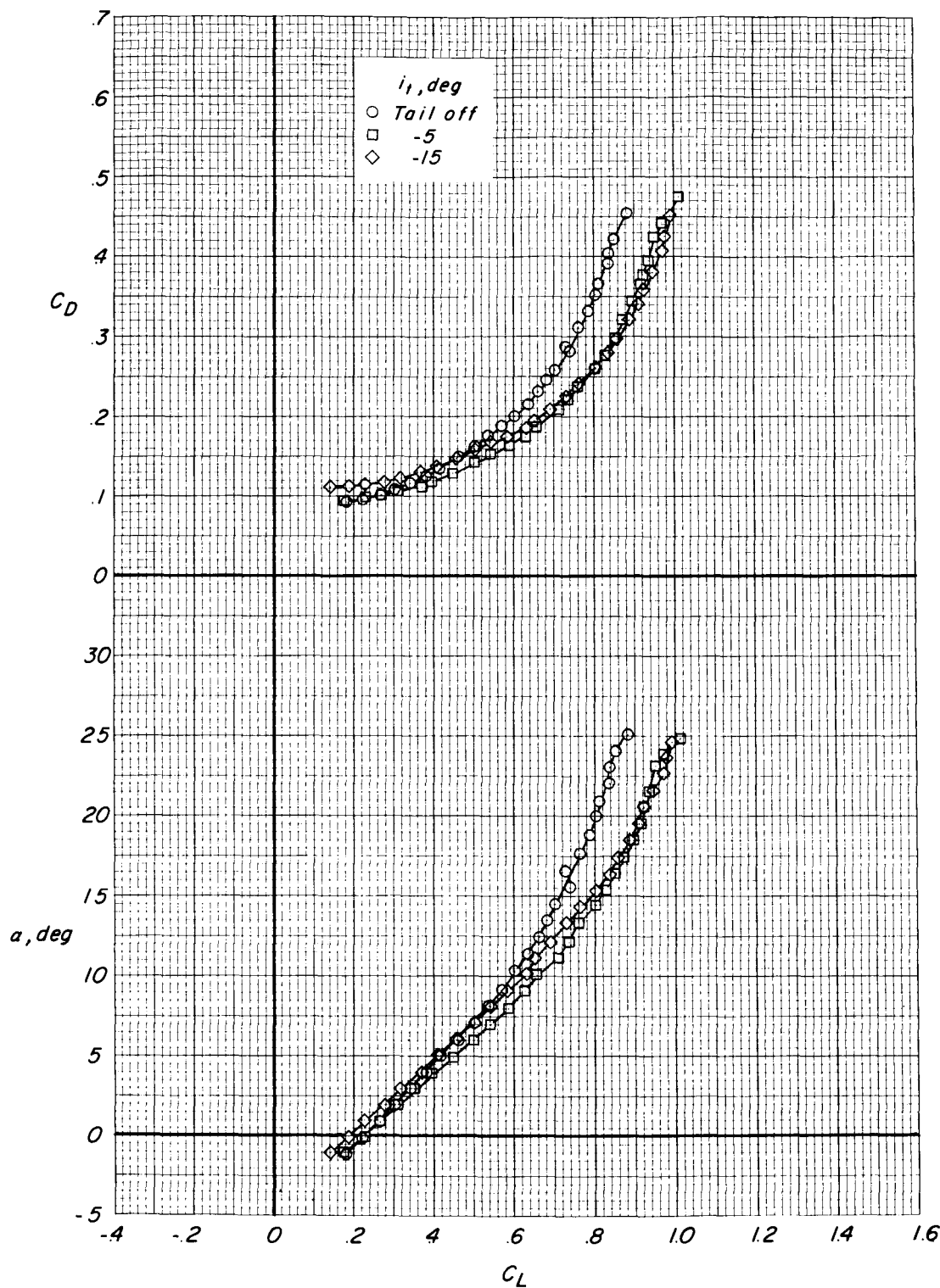
Figure 5.- Aerodynamic characteristics in pitch of the model with leading-edge and trailing-edge flaps deflected. $\delta_f = 45°$; $\delta_n = 30°$.
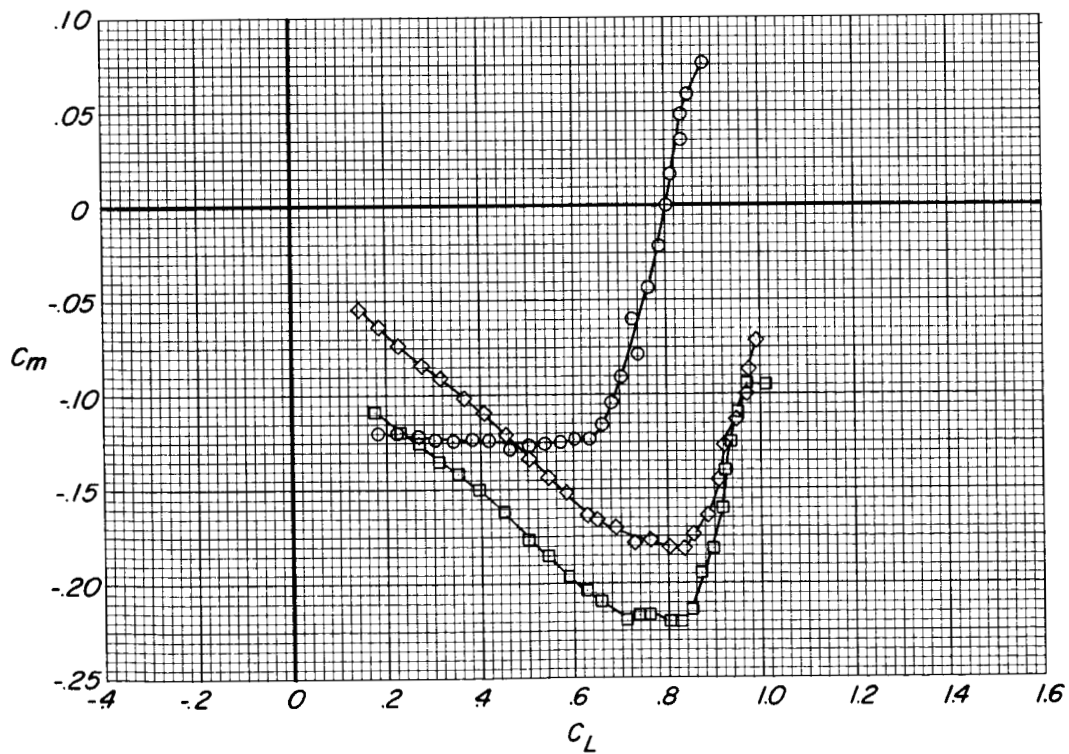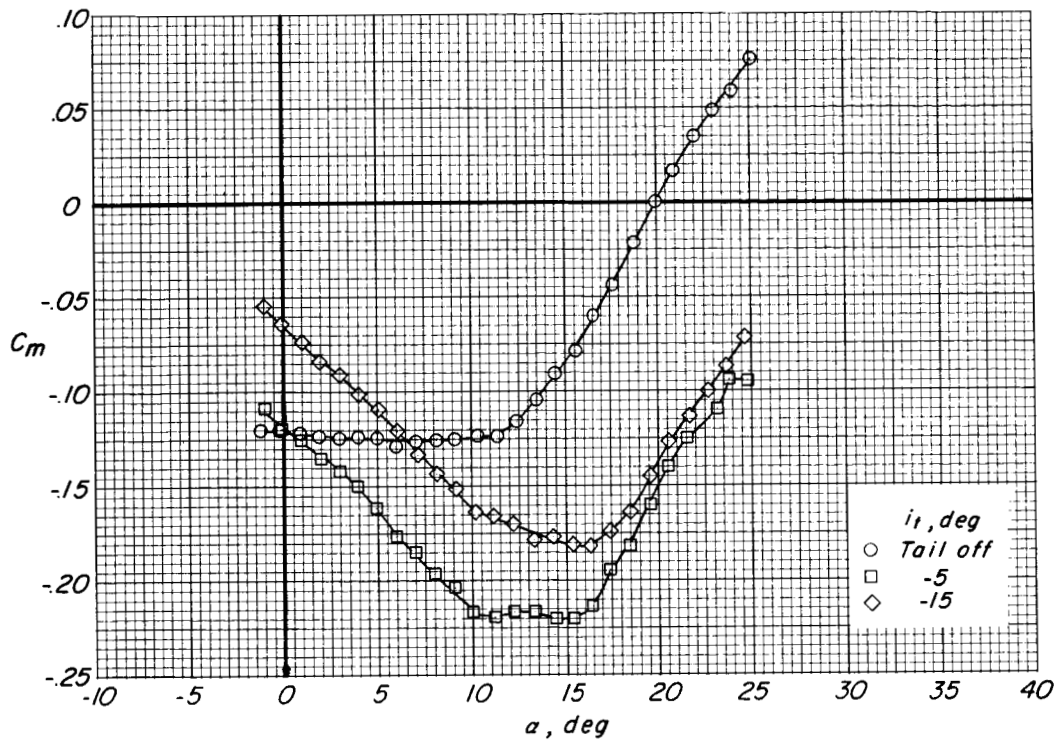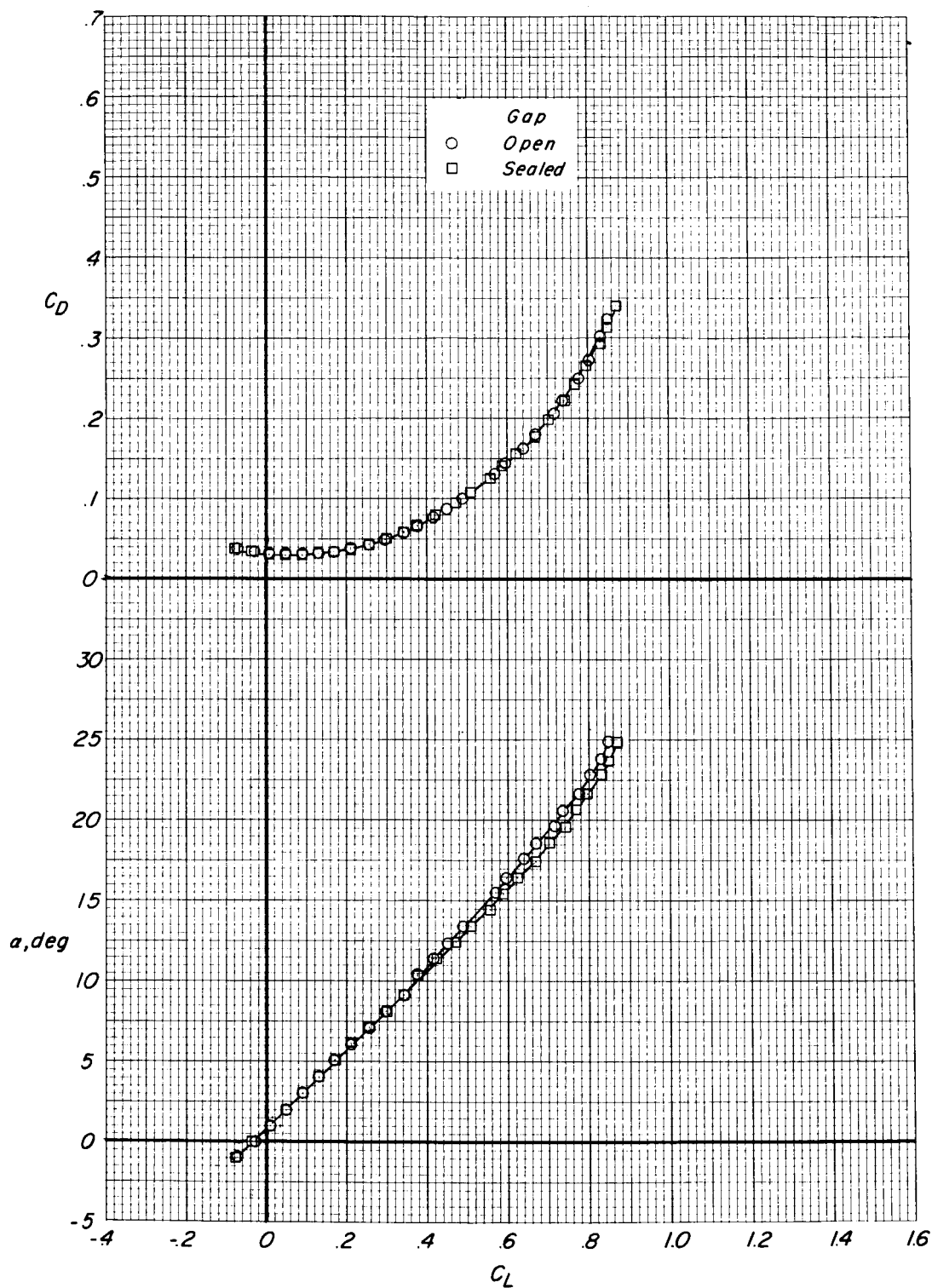
Figure 5.- Concluded.
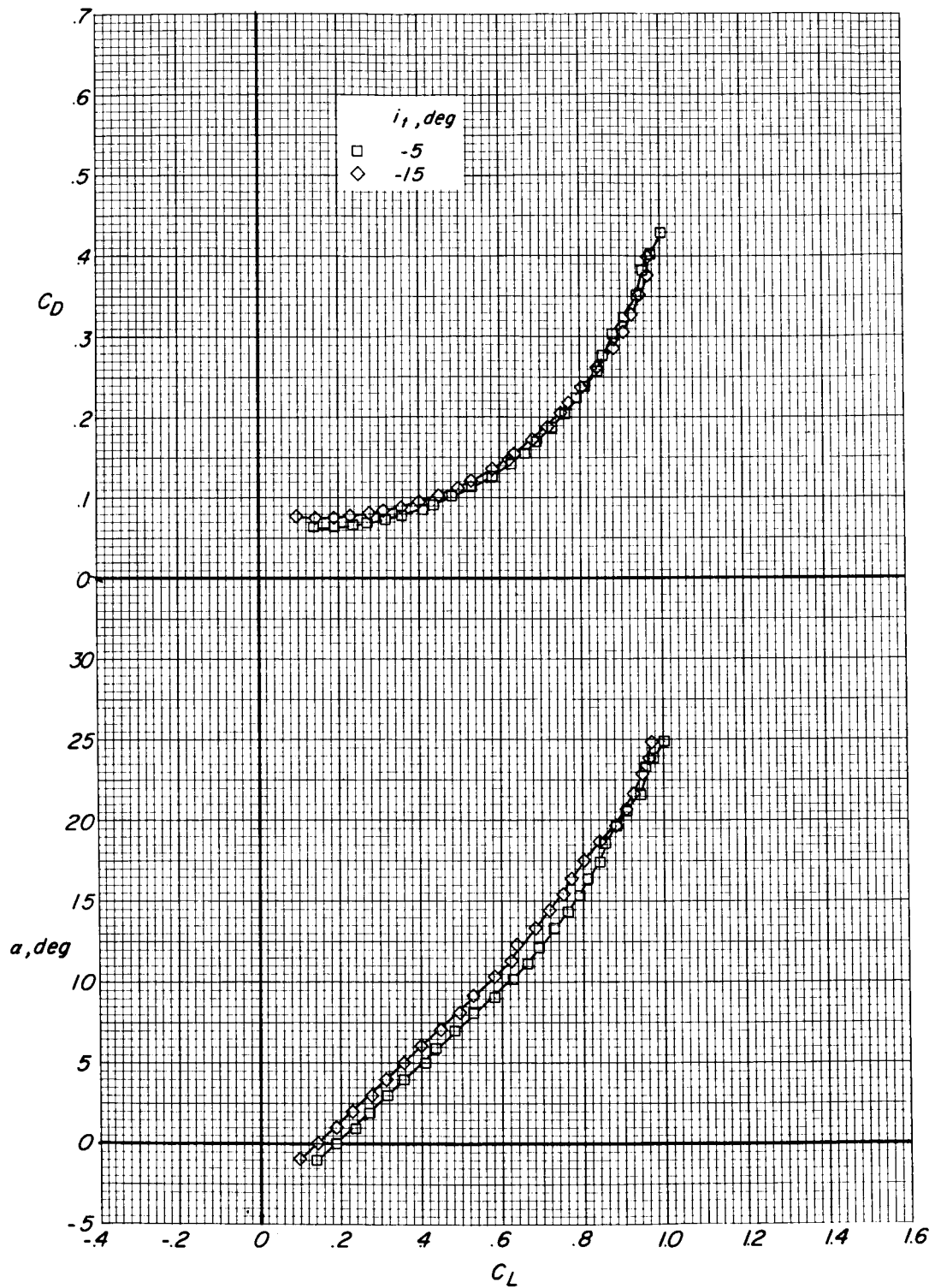
Figure 6.- Aerodynamic characteristics in pitch of the model with leading-edge and trailing-edge flaps deflected. $\delta_f = 30°$; $\delta_n = 30°$.

Figure 6.- Concluded.

Figure 7.- Effect of sealing the gap at the wing leading-edge flaps on the aerodynamic characteristics in pitch of the model. $\delta_f = 0°$; $\delta_n = 30°$; $i_t = -5°$.
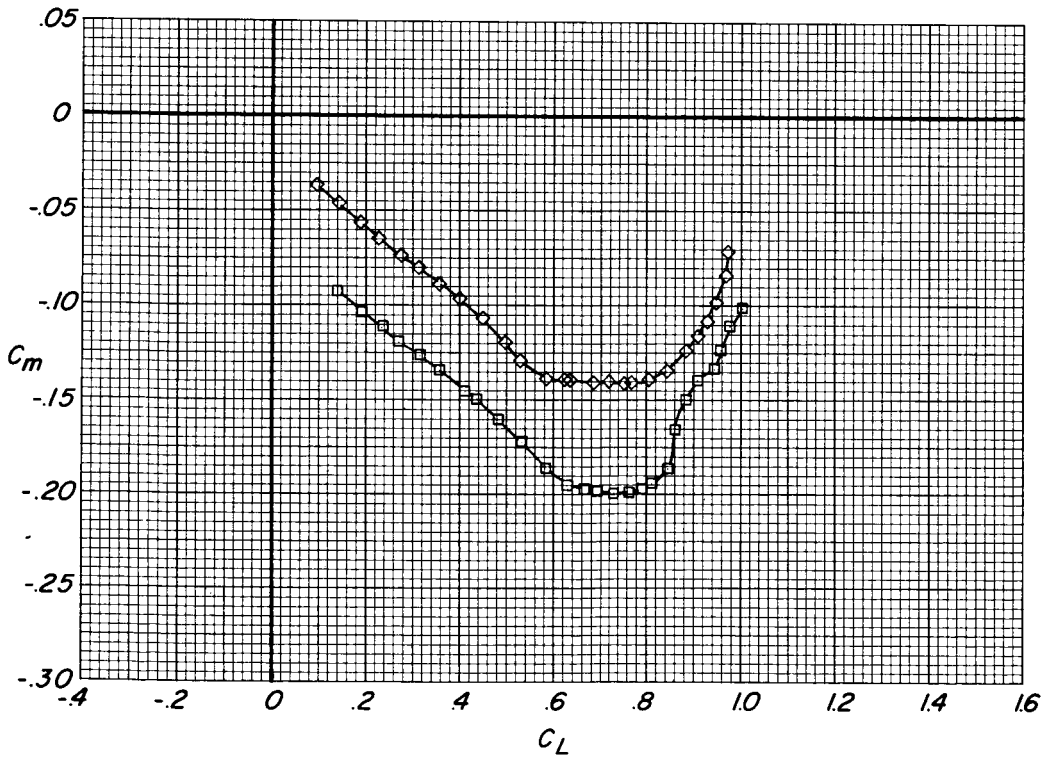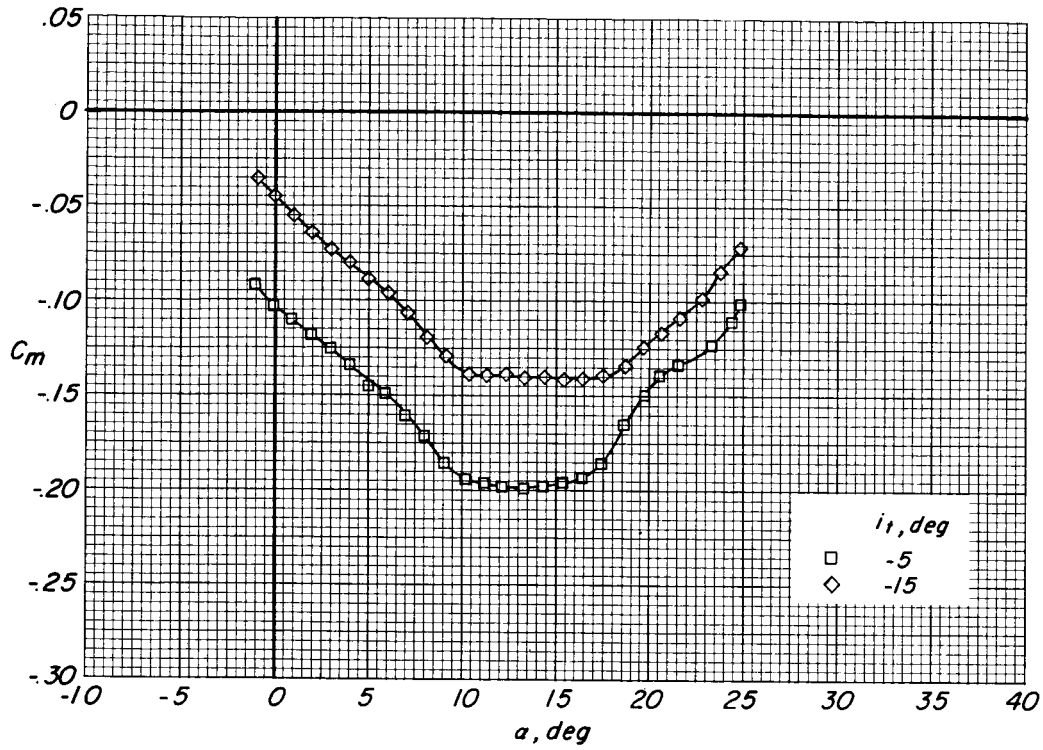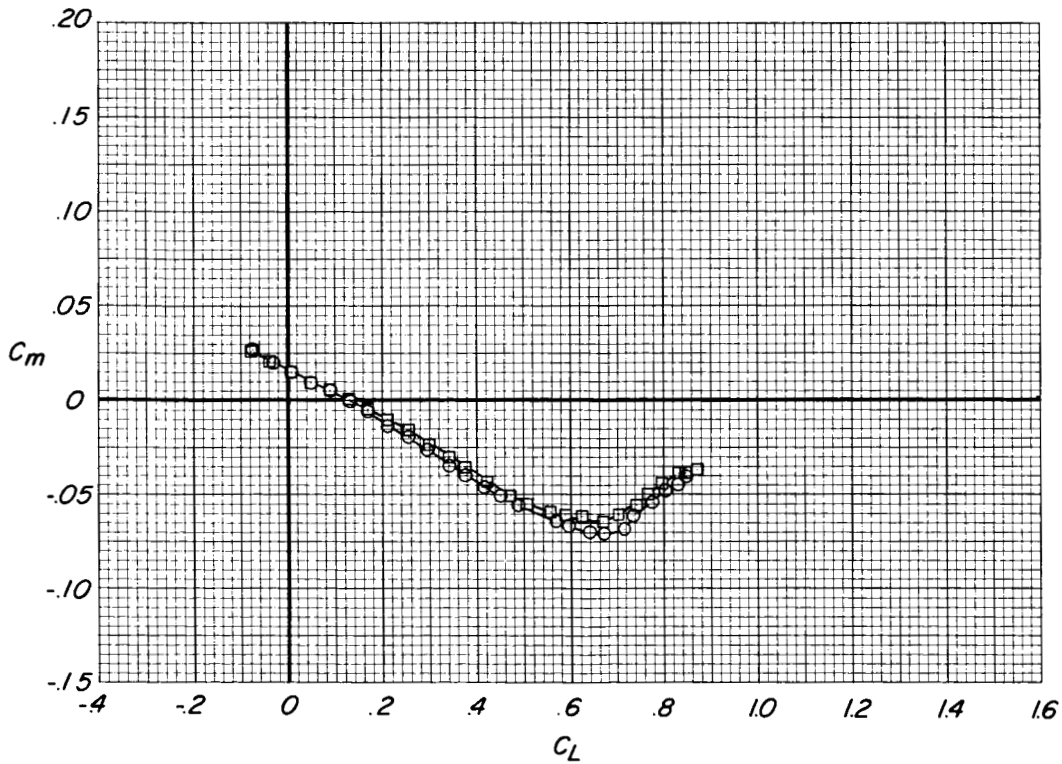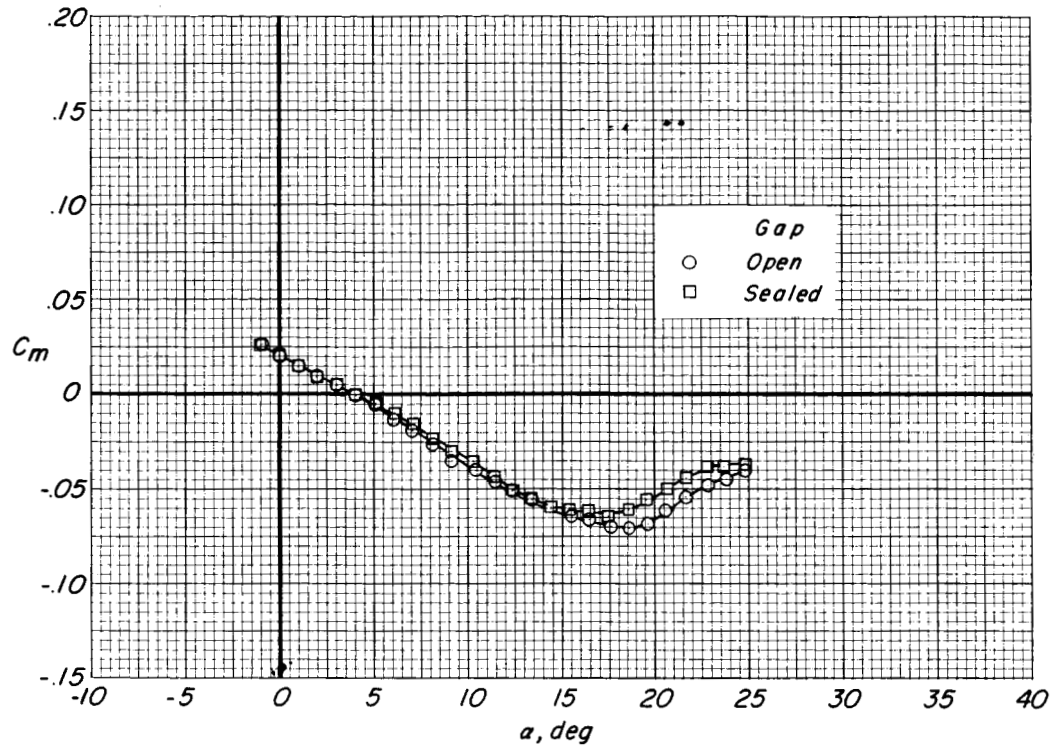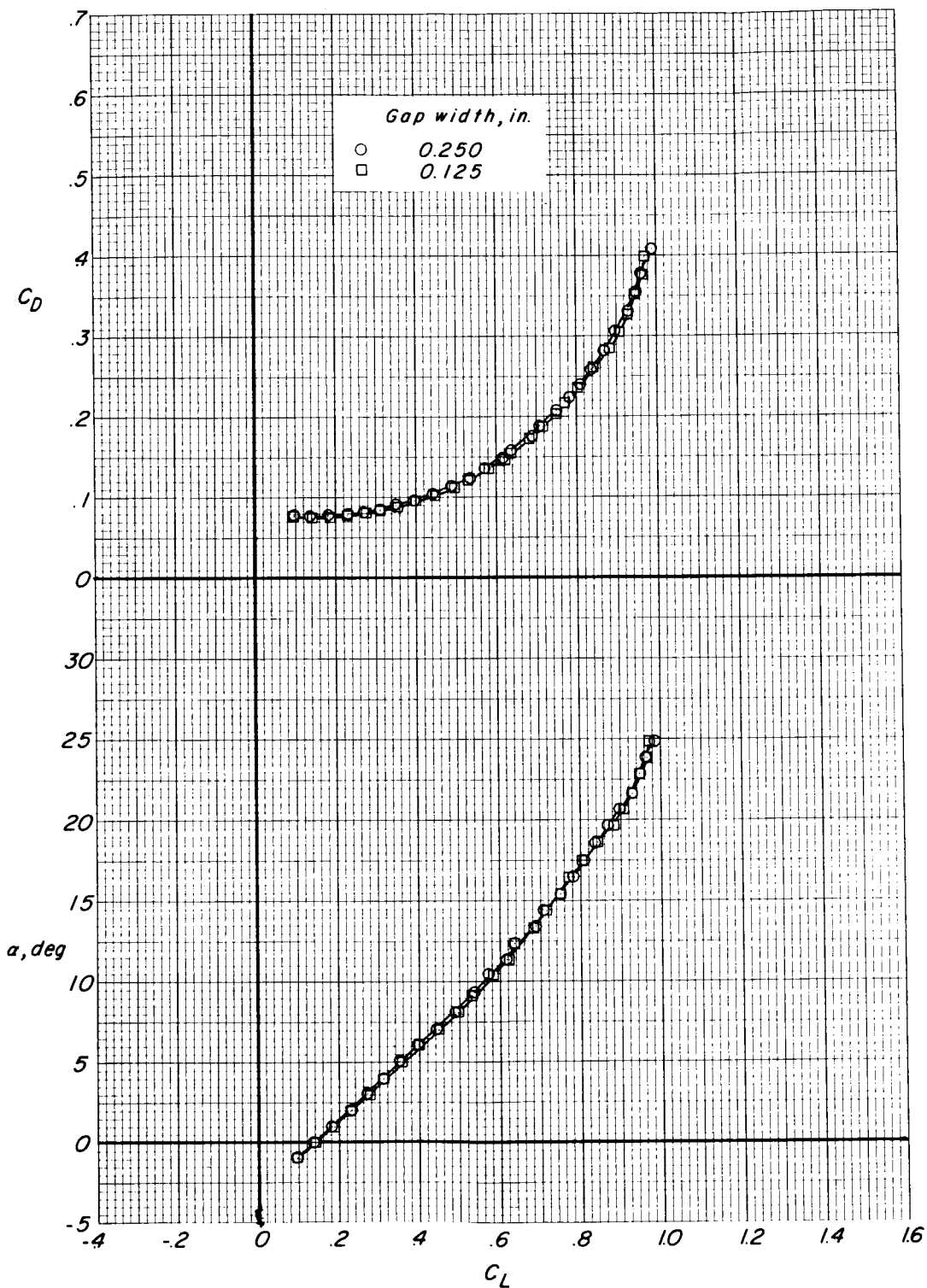
Figure 7.- Concluded.

Figure 8.- Effect of gap width at the trailing-edge flaps on the aerodynamic characteristics in pitch of the model with the leading-edge flaps deflected. $\delta_f = 30°$; $\delta_n = 30°$; $i_t = -15°$.

Figure 8.- Concluded.
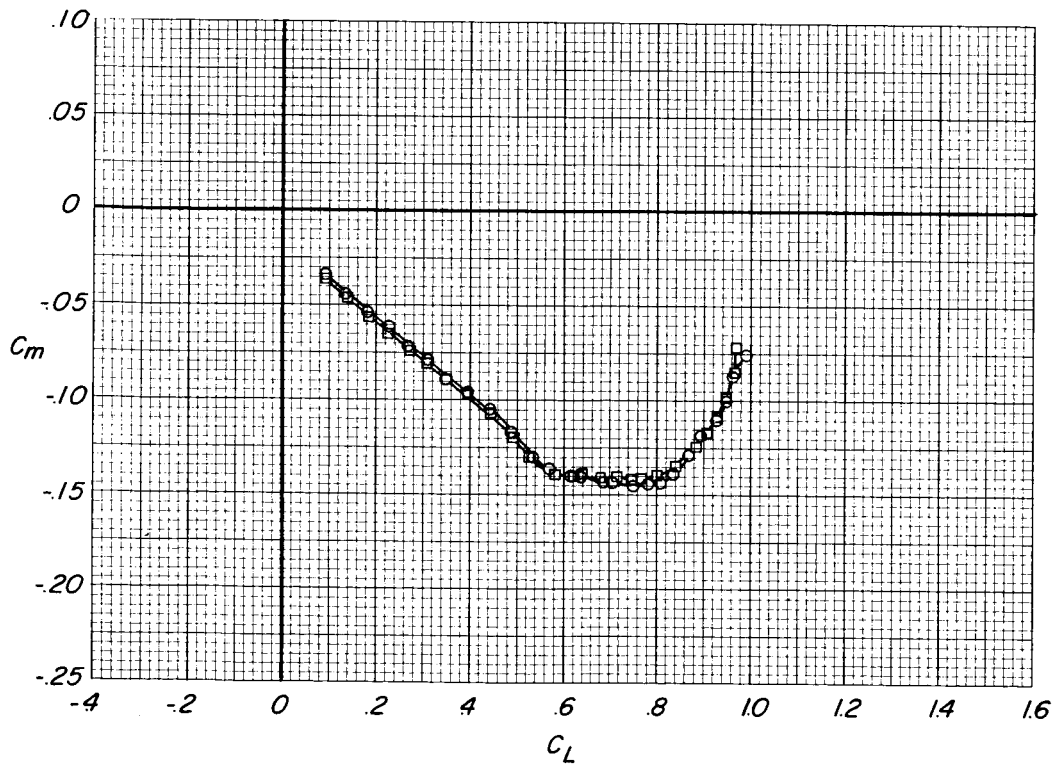
C_{Y_β}

0

-.01

-.02

-.03

δ_n, deg

○   0
□   30

.008

.006

C_{n_β} .004

.002

0

0

-.002

C_{l_β}

-.004
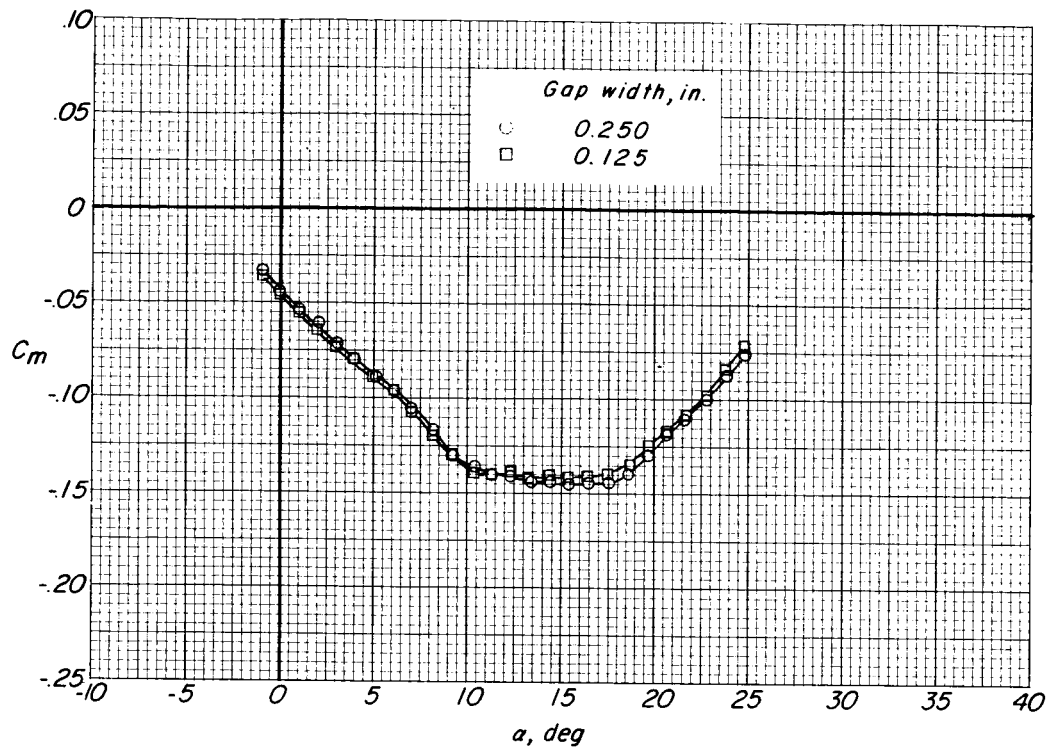
-.006

-.008

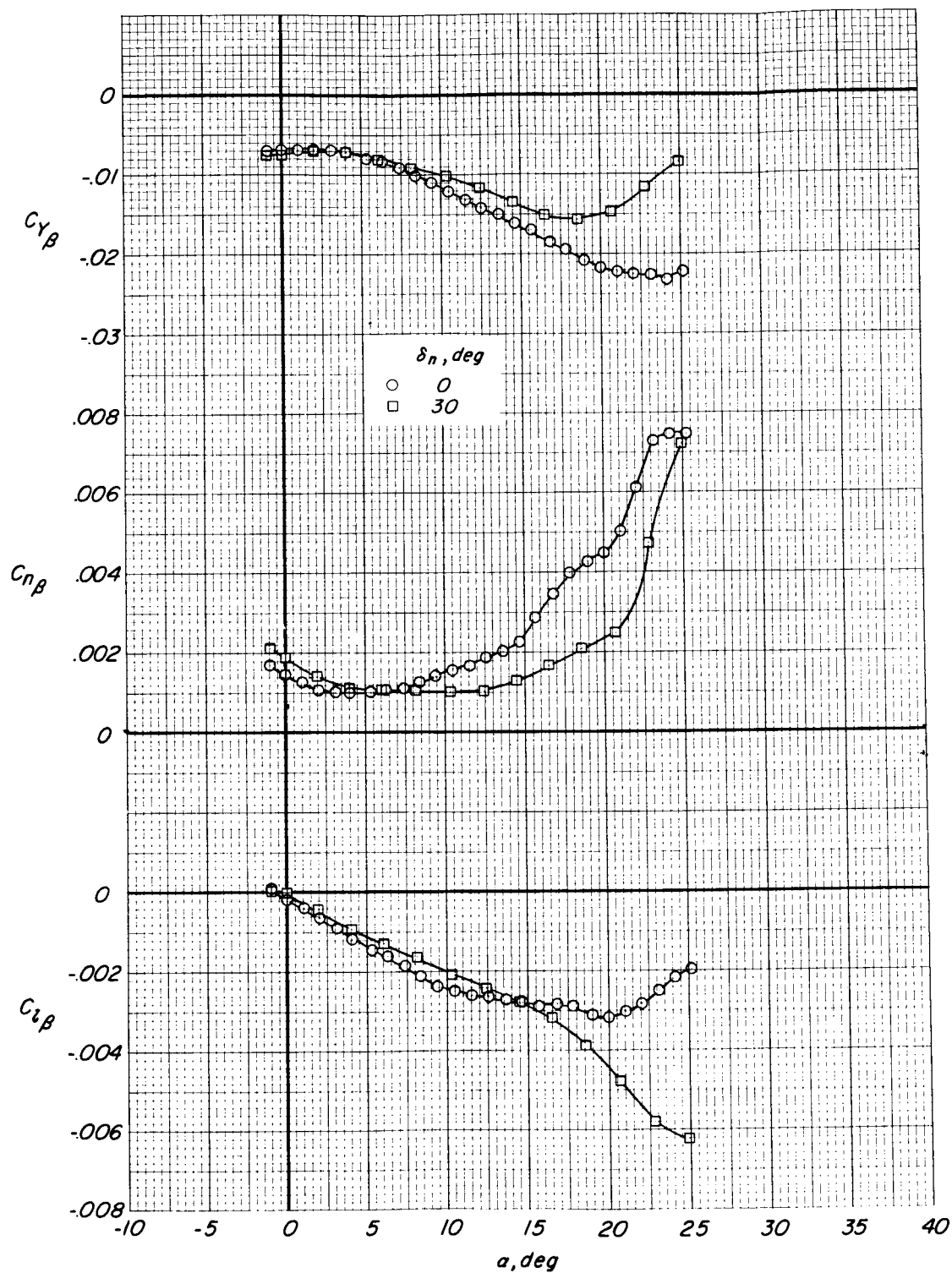-10   -5   0   5   10   15   20   25   30   35   40

a, deg

Figure 9.- Effect of leading-edge flap deflection on the lateral stability derivatives of the model. $\delta_f = 0^\circ$; $i_t = -5^\circ$.